Proceedings of ME 59001
Independent Study: Computational Fluid Dynamics
CCNY Summer 2023
August 6, 2023, New York City, NY, USA

ISCFD2023-0001

FLOW PAST A CIRCULAR CYLINDER: DATA VALIDATION

Hai Lu Lin[1]

[1]The City College of New York, New York, NY

ABSTRACT

An external flow past a circular cylinder is simulated in two dimensions using Nek5000 at Reynold's numbers 20 and 100. The simulation results are validated against published reference data and showed good agreement. It was found that the flow at Re 20 is symmetric while the flow for Re 100 oscillates passing through the cylinder. The flow near the front of the cylinder remains similar for both Reynold's numbers. The drag coefficient was found to be lower for Re 100, with a drag coefficient of 1.34, compared to a drag coefficient of 2.044 for Re 20. The pressure coefficients along the top surface of the cylinder are found to be the highest towards the front of the cylinder and lowest towards the middle of the cylinder. The pressure coefficients are also found to be lower for Re 100 than Re 20.

Keywords: external flow, circular cylinder, Nek5000

NOMENCLATURE

C_D	drag coefficient
C_P	pressure coefficient
Re	Reynold's number
Ux	x-direction velocity

1. INTRODUCTION

Flow past a circular cylinder is one of the most studied concepts in fluid dynamics. In this paper, flow past a circular cylinder in two-dimensions is simulated at Reynold's numbers 20 and 100 using Nek5000. The streamlines, pressure contours, and vorticity contours will be studied to better understand the flow around the cylinder. The drag and pressure coefficients will also be studied. The results will then be validated against the already published reference data.

2. MATERIALS AND METHODS

The simulations in this paper are run using Nek5000, a spectral element computational fluid dynamics code. To set up the simulations, a 100 by 50 rectangular mesh is created using Gmsh, a mesh generator software. The circular cylinder is located at the center of the rectangular mesh and has a diameter of 1. The long rectangular mesh allows for the flow upstream of the cylinder to be undisturbed by the cylinder and also allows for a view of the effects of the cylinder on the flow past the cylinder. The mesh consists of 3480 quadrilateral elements, with a finer mesh in areas closer to the cylinder. Quadrilateral elements are used since Nek5000 only supports quadrilateral/hexahedral elements. The mesh used is shown in Figure 1.

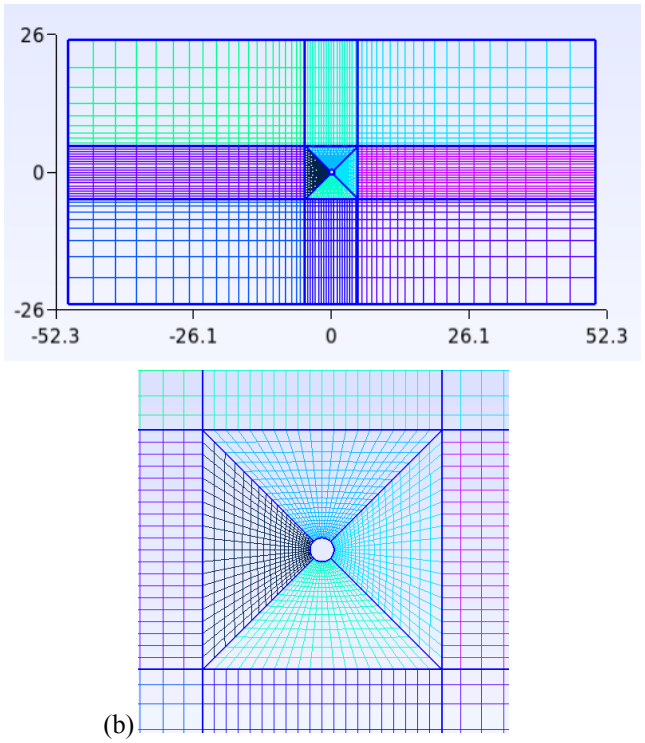

FIGURE 1: 100 x 50 mesh with quadrilateral elements: (a) full view and (b) close view.

For the boundary conditions, the left boundary is an inlet with a velocity Ux of 1, the right boundary is an outlet, the top and bottom boundaries are symmetry, and the cylinder is a wall.

The density of the fluid is also set to 1. Setting the diameter of the cylinder D, velocity U, and density ρ to be 1 allows for the simulations to be nondimensionalized. The Reynold's numbers are then adjusted to run the simulations at Re 20 and Re 100, using the equation

$$Re = \frac{\rho UD}{\mu}. \quad (1)$$

The boundary conditions and setup are shown in Figure 2.

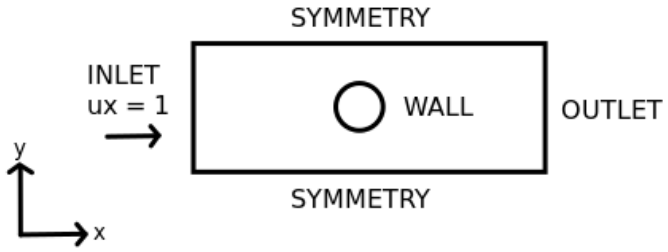

FIGURE 2: Schematic of the mesh and its boundary conditions.

To obtain the drag force needed to calculate the drag coefficient, the drag force calculations are implemented in the user routines file. The drag coefficient is then calculated using

$$C_D = \frac{2F_D}{\rho AU^2}. \quad (2)$$

For the pressure coefficients along the top of the cylinder, a set of 19 history points are implemented in the history file. The points are located along the top of the cylinder and are spaced at intervals of 10 degrees, ranging from 0 to 180 degrees from the front edge of the cylinder. The angle θ is shown in Figure 3. The pressure is monitored and recorded at these points. The pressure coefficient is then calculated using

$$C_P = \frac{p - p_\infty}{\frac{1}{2}\rho U^2}. \quad (3)$$

For the streamlines, pressure contours, and vorticity contours, they are visualized using Paraview.

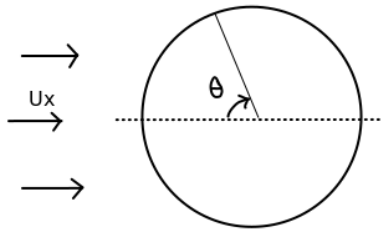

FIGURE 3: Edge point angle (deg) for the pressure coefficient.

3. RESULTS AND DISCUSSION

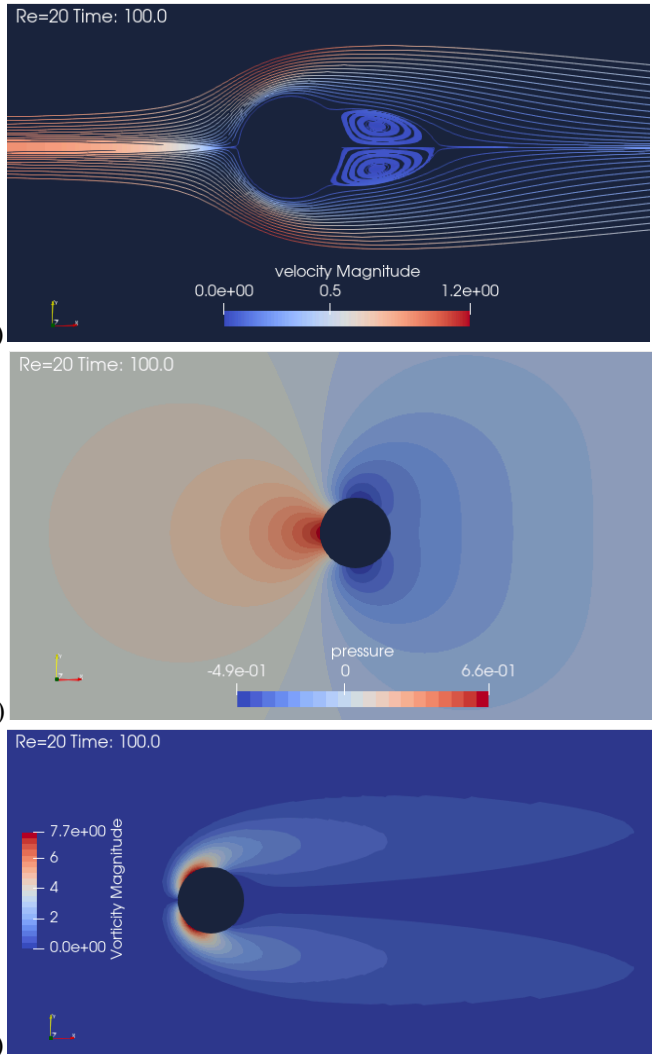

FIGURE 4: (a) Streamlines, (b) pressure contours, and (c) vorticity contours at Re=20.

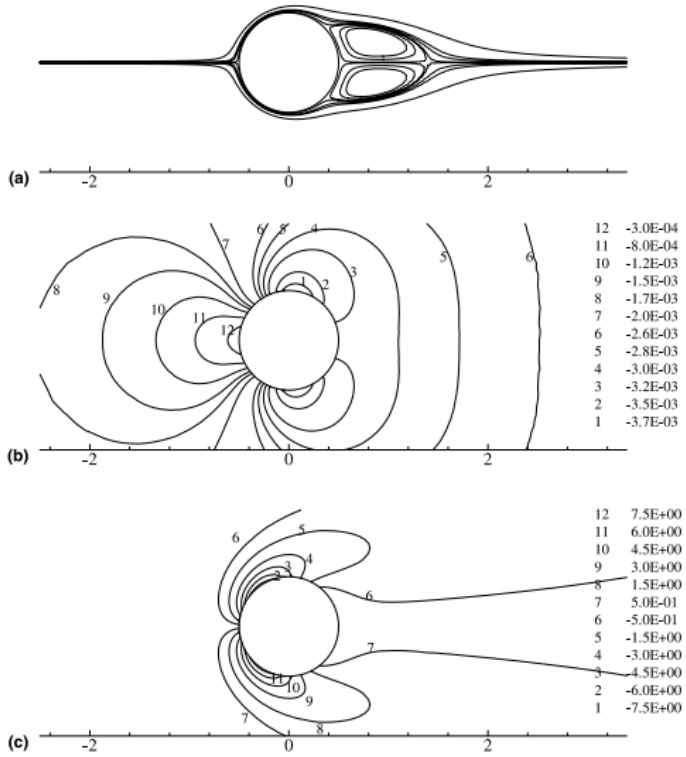

FIGURE 5: (a) Streamlines, (b) pressure contours, and (c) vorticity contours at Re=20 from Lee et al. [1].

For Re=20, the streamlines shown in Figure 4a are in good agreement with the reference streamlines shown in Figure 5a. From the streamlines, a pair of symmetric vortices can be seen forming behind the cylinder in the wake region where flow separation occurs. The pressure contours are also in good agreement with the reference pressure contours, shown in Figure 4b and Figure 5b respectively. From the pressure contours, there is a high pressure region at the front of the cylinder and 2 low pressure regions at the rear of the cylinder, one at the top and one at the bottom. Both the highest and lowest pressures occur on the surface of the cylinder. For the vorticity contours, the simulation results and the reference data are also in good agreement, shown in Figure 4c and Figure 5c respectively. Regions of high vorticity can be seen towards the front of the cylinder on both the top and the bottom. From the streamlines, pressure contours, and vorticity contours, the top and bottom of the cylinder both show symmetric results.

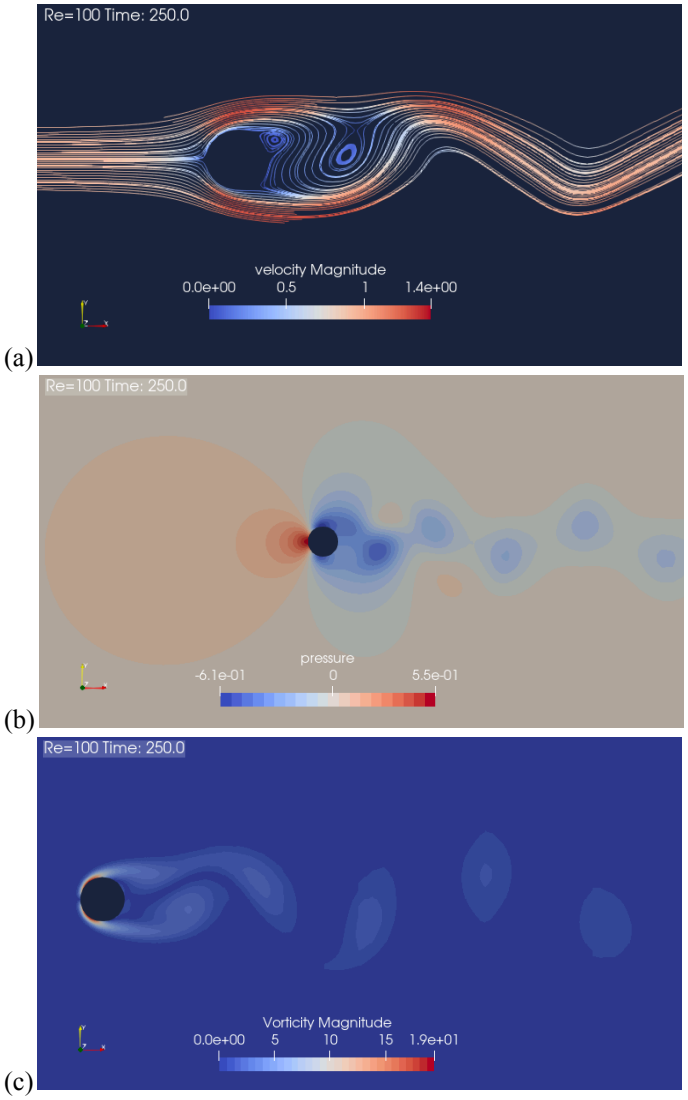

FIGURE 6: (a) Streamlines, (b) pressure contours, and (c) vorticity contours at Re=100.

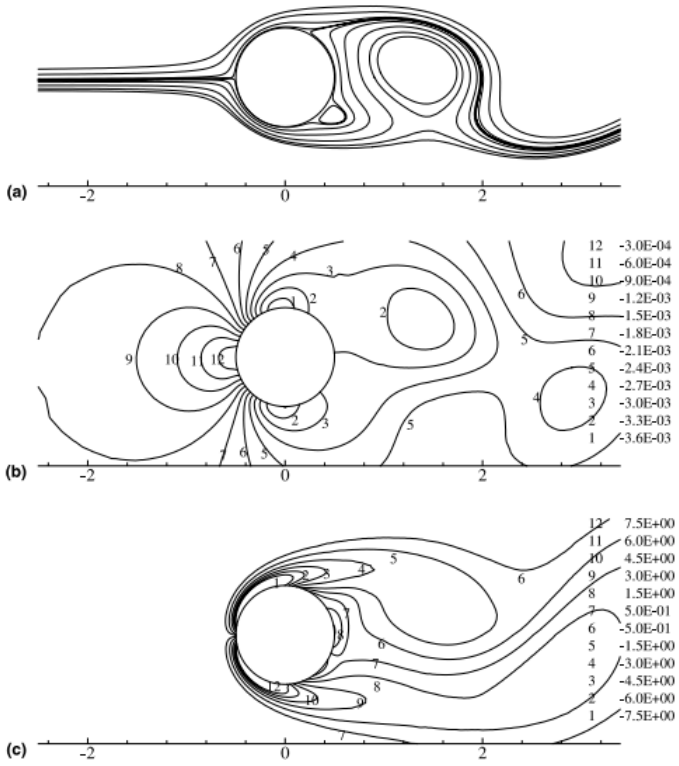

FIGURE 7: (a) Streamlines, (b) pressure contours, and (c) vorticity contours at Re=100 from Lee et al. [1].

For Re=100, the flow begins to oscillate past the cylinder. From the streamlines shown in Figure 6a, vortices can be seen forming trailing after the cylinder within the oscillating flow. From the pressure contours shown in Figure 6b, a region of high pressure is located in front of the cylinder while oscillating regions of low pressure trail behind the cylinder. From the vorticity contours shown in Figure 6c, regions of high vorticity can be seen towards the front of the cylinder on the top and the bottom. Regions of low vorticity also oscillate, trailing behind the cylinder and decreasing in magnitude further away from the cylinder. The streamlines, pressure contours, and vorticity contours are also in good agreement with the reference data shown in Figure 7, but the simulation results show the flow during a different state in oscillation compared to the reference data.

Comparing the simulation results for Re=20 and Re=100, both the regions of high pressure and high vorticity are similar. However, the streamlines, pressure contours, and vorticity contours are fixed and symmetric for Re=20, while the Re=100 streamlines and contours show oscillation.

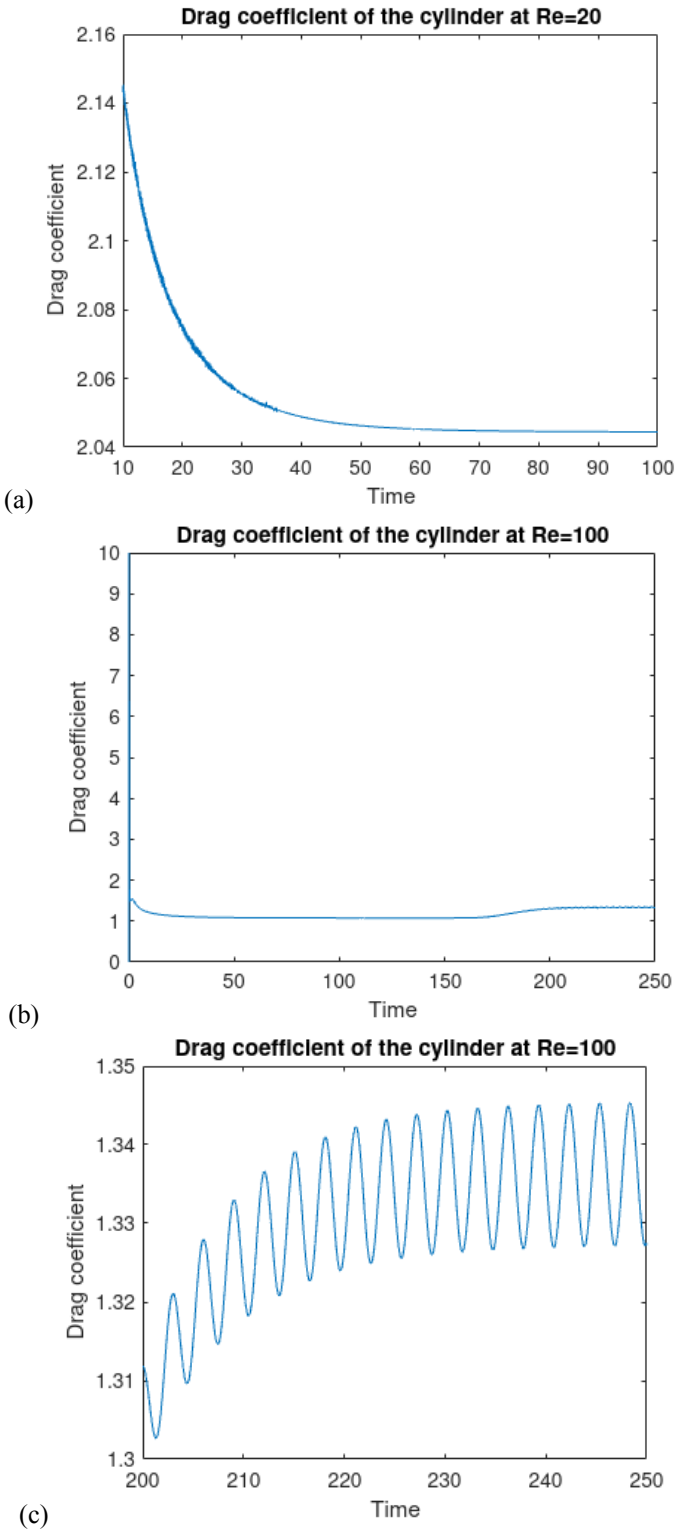

FIGURE 8: Drag coefficient of the cylinder over time at (a) Re=20, (b) Re=100, and (c) Re=100 close up.

Authors	C_D at Re=20	max C_D at Re=100
Beaudan et al. [2]	2.05	1.365
Present results	2.044	1.345

TABLE 1: Comparison of the drag coefficient for flow past a circular cylinder at Re = 20 and Re = 100.

Figure 8a shows the convergence of the drag coefficient of the cylinder over time for Re=20, meaning that steady state has been reached. The resulting drag coefficient for Re=20 is 2.044, which is in fairly good agreement with the reference drag coefficient of 2.05, with only a percent difference of 0.44%. For Re=100, the drag coefficient appears to approach a certain value as shown in Figure 8b, but a closer view in Figure 8c shows that the drag coefficient begins to oscillate. This could be due to the vortex shedding that occurs for Re=100. The maximum drag coefficient is 1.345, which is also in good agreement with the reference data of 1.365, with a percent difference of 1.47%. Between Re=20 and Re=100, the maximum drag coefficient for Re=100 is much lower than the drag coefficient for Re=20. The drag coefficients obtained from the simulation and the reference data are shown in Table 1.

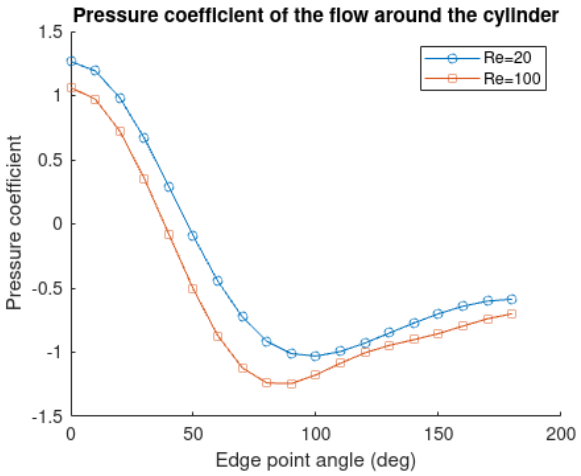

FIGURE 9: Pressure coefficient of the flow around the cylinder at Re=20 and Re=100.

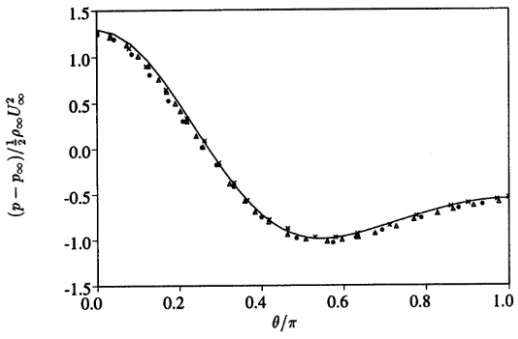

(a)

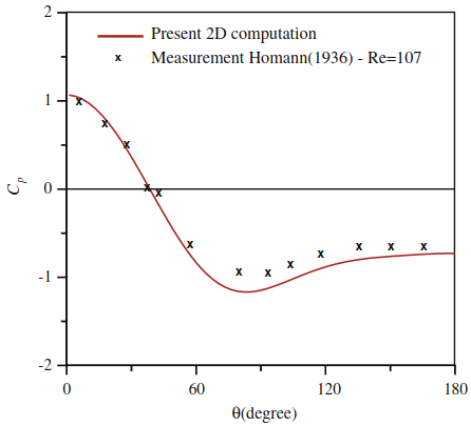

(b)

FIGURE 10: Pressure coefficient of the flow around the cylinder at (a) Re=20 from Beaudan et al. [2] and (b) Re=100 from Rajani et al. [3].

The pressure coefficients along the top surface of the cylinder are shown in Figure 9 for both Re=20 and Re=100. For both Reynold's numbers, the pressure coefficient is at its highest at 0 degrees at the front of the cylinder and decreases until it reaches a minimum, which then begins to increase slightly as it reaches the rear of the cylinder. The overall pressure coefficient along the top surface of the cylinder is lower for Re=100 compared to Re=20. Comparing the pressure coefficients to the reference data shown in Figure 10, both the simulation and reference data for Re=20 appear to have a maximum of about 1.25 and a minimum of about -1, showing good agreement. For Re=100, both the simulation and reference data appear to have a maximum of about 1 and a minimum of about -1.25, which also show good agreement. However, due to a lack of access to the exact data points from the reference sources, the comparisons are rough approximations.

4. CONCLUSION

In this paper, the simulation results from Nek5000 were validated against published reference data and showed good agreement between the simulation results and the reference data. We were able to compare the overall flow pattern using streamlines, pressure contours, and vorticity contours, as well as comparing the drag and pressure coefficients. The overall difference between Re=20 and Re=100 is that the flow for Re=20 is steady and symmetric while the flow for Re=100 oscillates. The drag and pressure coefficients are also lower for Re=100.

ACKNOWLEDGEMENTS

I would like to thank Professor Taehun Lee for giving guidance on numerous aspects of this work as well as Margulan Tursynkhan and Timothy Khusial for their support in understanding the Nek5000 output configuration.

REFERENCES

[1] Lee T, Lin C-L. “An Eulerian Description of the Streaming Process in the Lattice Boltzmann Equation.” *Journal of Computational Physics*, vol. 185, no. 2, 2003, pp.445–471.

[2] Beaudan P, Moin P. “Numerical experiments on the flow past a circular cylinder at sub-critical Reynolds number.” Ph.D Thesis, Stanford University, 1994.

[3] Rajani B.N., et al. “Numerical Simulation of Laminar Flow Past a Circular Cylinder.” *Applied Mathematical Modelling*, vol. 33, no. 3, 2009, pp. 1228–1247.